A novel compact 3D laser-sintered collimator for neutron scattering

A novel compact 3D laser-sintered collimator for neutron scattering.

Christopher J. Ridley,[1,2,a)] Pascal Manuel,[2] Dmitry Khalyavin,[2] Oleg Kirichek,[2] and Konstantin V. Kamenev[1]
[1)] *The School of Engineering and the Centre for Science at Extreme Conditions, The University of Edinburgh, Peter Guthrie Tait Road, Edinburgh EH9 3FD, UK*
[2)] *ISIS Facility, Rutherford Appleton Laboratory, Chilton, Didcot OX11 0QX, UK*

(Dated: 14 September 2015)

Improvements in the available flux at neutron sources is making it increasingly feasible to obtain refineable neutron diffraction data from samples smaller than 1 mm^3. The signal is typically too weak to introduce any further sample environment in the $30 - 50$ mm diameter surrounding the sample (such as the walls of a pressure cell) due to the high ratio of background to sample signal, such that even longer count times fail to reveal reflections from the sample. Many neutron instruments incorporate collimators to reduce parasitic scattering from the instrument and from any surrounding material and larger pieces of sample environment, such as cryostats. However, conventional collimation is limited in the volume it can focus on due to difficulties in producing tightly spaced neutron-absorbing foils close to the sample, and in integrating this into neutron instruments. Here we present the design of a novel compact 3D rapid-prototyped (or 'printed') collimator which removes these limitations, and is shown to improve the ratio of signal to background, opening up the feasibility of using additional sample environment for neutron diffraction from small sample volumes. The compactness and ease of customisation of the design also allows this concept to be integrated with existing sample environment, and with designs that can be tailored to individual detector geometries without the need to alter the setup of the instrument. Results from online testing of a prototype collimator are presented. The proof of concept shows that there are many additional collimator designs which may be manufactured relatively inexpensively, with a broad range of customisation, and geometries otherwise impossible to manufacture by conventional techniques.

I. INTRODUCTION

Currently achievable levels of flux for neutron diffraction are orders of magnitude lower than those achievable with x-rays, meaning that sample sizes need to be larger to achieve sufficient diffraction statistics in a reasonable time-frame. However, the high penetrability of neutrons makes them uniquely well suited for the study of bulk material properties, whilst their intrinsic spin allows them to be used to characterise magnetic structures.

Although there is a significant amount of science that is possible with neutrons within these sample limitations, it is not always feasible to use or produce large samples. For example, sample volume limits the achievable pressures due to pressure cell limitations[1]. This indirectly limits other external parameters applicable such as the temperature or magnetic field. Some samples may be challenging to synthesise in large quantities as a powder, or may not form sufficiently large single crystals (as is the case with zeolites[2]). Single crystal diffraction contains information that powder samples lose due to orientation averaging.

Improvements in neutron detection, and in the production of neutrons at large facilities, makes it sometimes possible to secure data from samples of a few mg with certain instruments. To distinguish the sample data above the background it is important to mask as many sources of background from the instrument and auxiliary equipment as possible. This is typically achieved using 'beam scrapers' or slits to narrow the incident beam, and collimators to focus the detectors on a reduced volume of space in the sample area. For example, this principle is used extensively on the instrument Engin-X at the ISIS Facility[3], allowing the volume of space visible to the detectors (gauge volume) to be reduced to 0.5x0.5x0.5 mm^3, so that detailed strain profiles within large samples can be obtained. Conventional collimators are limited in how small the gauge volume can be by the length of the collimator, the minimum possible proximity to the sample, the maximum number of slits that can be accommodated, and the space available within the instrument (see figure 1). Instruments also need versatility with collimation, to allow for different types of measurement, sample sizes, and sample environments. The collimators used to vary the gauge volume on Engin-X are bulky, and difficult to align, such that most instruments tend to use collimation with larger gauge volumes which remain fixed in place, or which oscillate about a fixed point to reduce shadowing effects.

Conventional neutron collimators use thin foils, typically made from mylar, aluminium or stainless steel, coated in an absorbing material, such as gadolinium or enriched boron, to absorb divergent incident neutrons, or those scattered from unwanted sources. The foils are held together, and tensioned to ensure uniformity, using bolted frames. The unit for gripping and tensioning the foils limits how closely they may be placed together, their angular separation, their proximity to the sample,

[a)] c.ridley@ed.ac.uk

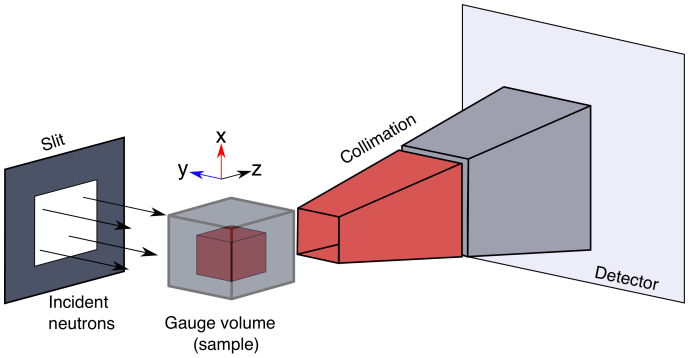

FIG. 1. Schematic showing the gauge volume defined using a slit to narrow the incident beam, and a collimator to narrow the diffracted path. As shown, the size of the gauge volume can be reduced if the collimator is longer, or closer to the sample. The gauge volume can be reduced further if additional vertical foils are inserted within the collimator. In reality the gauge volume is not sharply defined as in the figure, but has a gaussian intensity profile in 3D.

and therefore the efficiency of the collimator. Modelling software, in combination with ray tracing simulations, show that there are designs which can greatly improve the performance of the collimator, but are not possible to implement using conventional assembly or machining techniques. Here we present the design and construction of a 3D rapid prototyped (printed) collimator, free from many of these constraints. The scale, and prospect for customisation, of the device means that the techniques presented can be applied to a broad range of applications. These include the design of interchangeable collimators for a particular neutron instrument, allowing a broader range of possible measurements, or for use in developing small scale pressure cells for neutron diffraction, which are currently hampered by high background[4].

II. EXISTING COLLIMATOR DESIGNS

For collimation of incident radiation, one of the simplest devices is an extended slit. The length and cross-section of the slit reduces beam divergence, improving the resolution of the instrument, but this must be balanced with the loss in intensity. If used at the detector side of the sample, the slit can be tapered to match the geometry of the detector. A more efficient device, known as a Soller, consists of tightly spaced coated foils or sandwiches of absorbing and transmitting foils which are stacked parallel either vertically or horizontally, reducing the intensity loss whilst controlling the divergence of the beam. A honeycomb pattern of foils may be used to control the divergence of the beam in two dimensions[5]. An alternative design uses micro-channel plates (MCP) made through drawing and fusing many cladded glass tubes together, and dissolving the glass leaving a grid of channels[6,7]. Honeycomb and MCP collimators offer much improved flux transmission, and allow for consistent collimation of larger beam sizes. The diameter of the MCP channels means that they need only be a fraction of the length of a honeycomb collimator to achieve the same collimation.

For the diffracted beam, depending on the detector and scattering geometry, collimators are usually radial type. A radial collimator consists either of a housing of angularly spaced foils, or a collection of Soller units angled around the sample. The former have fewer foils, so offer the best transmission to detector, but are consequently more limited in gauge volume. Sollers offer tighter collimation, at the expense of lost detector coverage due to the frame of the each Soller. Thin MCP collimators[8] may be installed close to the detectors, such as for imaging or transmission experiments, but require curvature to be effective for angular-dispersive diffraction. Whilst it is possible to introduce curvature to MCPs through 'slumping', there are few examples of this being implemented, possibly due to difficulties in manufacture. Honeycomb collimators are made from joined die-pressed foils, which currently cannot be manufactured with radial angular separation. 3D printing can overcome the limits of these conventional designs; Zhong *et al.*[9] present an elongated slit design, made from 3D printed W-Ni, for the collimation of hard X-rays in a modulation telescope. The device is large and uses broadly spaced 3 mm thick walls which would be inefficient for neutron scattering measurements. Here we present the design of a 3D printed near-sample radial collimator, with significantly thinner 0.1 mm wall sections, providing a compact method to reduce the gauge volume without the need to remove existing collimation from the neutron instrument.

III. 3D DIRECT METAL LASER-SINTERING

Direct metal laser sintering (DMLS) is an additive rapid-prototyping process whereby fine metallic powder is layered and sintered together in high precision using a laser source. The process takes a computer aided design, which is then sliced into multiple layers/planes. The powder is then sintered to match each layer, gradually building the full model. The finished part can be treated much like parts constructed using traditional techniques, being machined, ground, coated, and polished. Further information on the process, and a review of its development can be found elsewhere[10,11].

The advantages of this technique are that there is virtually zero material wasted, powder that is not sintered in the layer may be removed and reused, and that more complex geometries can be made without concerns due to tooling access. Curved profiles, thin wall sections, and tightly spaced components can be printed without added complexity. The precision of the printing can be as good as ± 0.05 mm, whilst the materials offered are varied; maraging, or stainless steels, aluminium and copper are commonly used. The minimum wall thickness

achievable depends on length of the feature, and the material it is made from. The minimum resolution typically offered commercially is 0.1 mm. Another advantage of laser sintering, unlike other plastic printing techniques, is the more consistent material properties of the finished part.

IV. COLLIMATOR DESIGN

The main objective of this work was to improve the signal-to-noise ratio from a sample volume of approximately 0.5 mm^3 housed in an opposed sapphire anvil pressure cell similar to that reported in the work of Jacobsen *et al.* [12]. In this cell the sample signal is very weak compared to the signal from the anvils, the gasket (used to contain the sample between the anvils), and the pressure cell itself. It is not possible to mask the sapphires or gasket without obscuring the sample. Due to the cryogenic purpose of this cell there were additional design constraints that needed to be met; firstly any additional material had to be of minimal mass so as to have as little effect on cooling times as possible; secondly that the device must fit within a 100 mm cryostat bore. Initially miniature conventional collimators were considered, but were either impossible to construct so close to the sample, and in such a confined space, or did not offer a fine enough collimation to offer improvement to the signal.

3D laser sintering offered the possibility to remove the need for tensioning systems, and also opened up the possibility of manufacturing a 2D radial collimator (curved in two planes radially), with angled foils positioned both vertically and horizontally. This may offer a considerable advantage over conventional 1D radial (curved in one plane) collimators, which do not discriminate signal from points along the axis of the collimator, and can be easily formed and angled in complex geometries unlike 2D MCP collimators. The main benefit of rapid-prototyping is that the specific shape and dimensions of the collimator can be easily customised to fit the pressure cell in question in the computer aided design stage. The specific shape and dimensions of the device can be easily customised in the computer aided design stage.

A. Simulation

To verify the feasibility of using such fine near sample collimation with limited collimator length, several simulations were performed using custom JAVA ray tracing code to visualise the gauge volume,[13] and Monte Carlo neutron ray tracing was performed using McStas[14,15] to estimate the possible improvement in sample signal.

The design of the pressure cell meant that the collimator can be no closer than 15 mm to the sample, and to ensure that the device would fit safely into the bore of the cryostat the length of the collimator should not exceed 30 mm. With these two parameters fixed JAVA

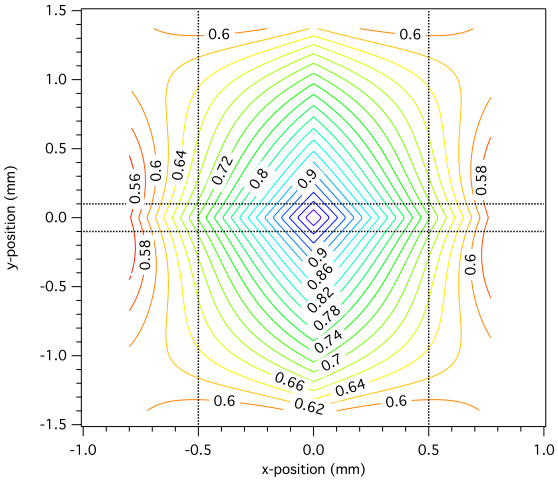

FIG. 2. Gauge volume profile in xy-plane (as defined in figure 1) of sample region as defined by two dimensional radial collimation. The sample region is defined by the dashed lines in the figure. The contour scale is relative to maximum solid angle at the central position of the collimator. The opening parameters were chosen to have a 4° horizontal separation, and a 6° vertical separation. The JAVA simulation assumes zero wall thickness.

ray tracing was used to determine the effect of number of collimator slits, and their angular spacing, on the gauge volume in the sample region. This was achieved through calculation of the visible solid angle at each point in the sample region using vector analysis and assuming zero wall thickness. If the material in the beam is assumed to be an isotropic scatterer, the solid angle may be thought of as a measure of the signal contribution. The simulation radially stacks a number of collimators similar in geometry to that shown in figure 1 summing the solid angle contributions from each at a given position in the sample volume. Figure 2 shows the calculated gauge volume profile chosen for the design of the collimator, with both vertical and horizontal collimation. The vertical collimation was designed to be broader than the horizontal collimation to allow for variations in the vertical position of the sample between the anvils. Integrating the drop in solid angle over the sample region shows that it falls to 86 % of the uncollimated value horizontally, and 95 % vertically. If the parameters of the collimator slits are altered to reduce the loss in solid angle in the sample volume, then there is a proportional increase in background signal from surrounding. Vertically this is less important, as this region can be effectively masked through narrowing the incident beam, this is less effective horizontally as the beam is directed straight through the gasket.

The effects of wall thickness have been calculated by Wang *et al.* [16], who found that the effect is non-negligible but small, reducing the maximum transmission of the collimator by as much as 15 %. The most efficient collimator will have a wall thickness just sufficient to ensure struc-

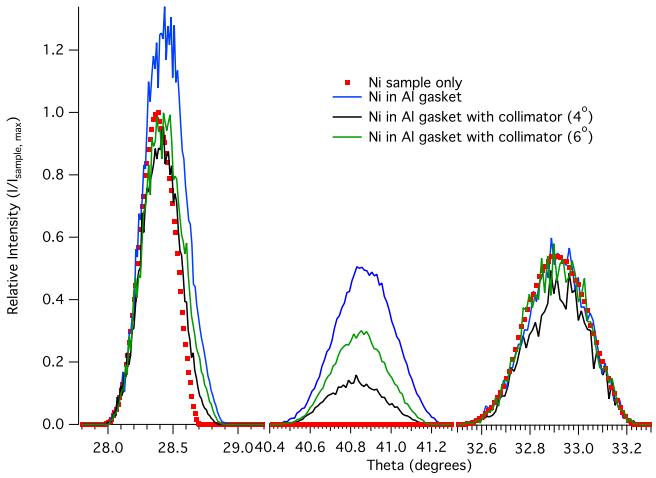

FIG. 3. McStas simulation results. The three peaks are (from left to right) sample with overlapping peak from gasket, gasket peak, sample peak without gasket contribution. Whilst the 4° collimator offers a reduction of gasket contribution to 20 % it also reduces the sample intensity. The 6° collimator reduces the gasket peak intensity by 50 % and negligibly reduces the sample intensity.

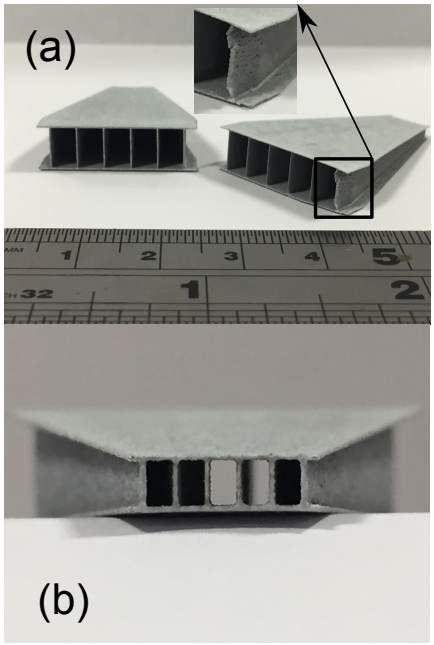

FIG. 4. Two of the stainless steel 316L printed test pieces painted with Gd-paint post thermal cycling (a) left, 0.2 mm wall thickness, right, 0.1 mm showing wall damage. (b) close view of sample side of 0.2 mm collimator.

tural stability, and no larger. This can be verified using the CAD model with other computational techniques such as finite-element analysis, prior to manufacture.

To make a quantified estimate for the level of reduction in background signal from the gasket, Monte Carlo ray tracing was performed using a simple McStas instrument. The instrument was modelled consisting of a source, cylindrical detector bank, and a beam stop behind the sample position. The sample was modelled as a cylinder of Ni powder 1 mm thick with 1 mm diameter, and the gasket as a hollow cylinder of Al powder with the same thickness but an outer diameter of 10 mm. The powder pattern was compared with just sample, sample with the gasket included, and sample with gasket and collimation included. The collimator was simulated with two different foil separations 4° or 6°, with an inner diameter of 30 mm and outer diameter of 92 mm. Incoherent scattering was neglected in these simulations to ease data comparison. The results are shown in figure 3.

B. Prototype construction and coating

3D printing does not guarantee that a part can be built successfully. The direction of the build in rapid prototyping will influence the likelihood of a successful build, and should be chosen so as to provide maximum support to the part as it is assembled. Long sections of thin wall segments may not build correctly as the material may not fuse together fully, or the laser may simply burn away excess material. Due to the potential length of the thin collimator walls it could not be predicted if construction would be possible. To find the minimum possible wall thickness that could be successfully printed, three test parts were trialled with wall lengths typical of the expected final design (approximately 5 mm) see figure 4. Printing of the parts was done with CRDM Ltd. Stainless steel 316L was chosen due to the improved strength over aluminium, which would be preferred for cryogenic applications. The 0.3 mm and 0.2 mm thick parts were built successfully, whereas the 0.1 mm thick part had some minor perforations on the wall section.

These prototypes were also used to test the coating process for the collimator. Due to the thin wall sections, and the desire to keep their thickness minimal, Gd-paint was chosen as the coating material. The parts were spray-coated with an approximate thickness of $\approx$ 25 µm by Euro Collimators Ltd. The coated test pieces were also used for thermal testing, as the collimator will eventually be cooled to sub-5 K temperatures in a cryostat, to ensure secure adhesion of the coating, and that the thermal stress on the system doesn't result in a structural failure. This was done through sudden and repeated immersion in liquid nitrogen. The parts were thermally cycled several times from ambient to nitrogen temperatures with no indication of the paint coming loose, or damage to the parts.

C. Final design

The test builds identified the optimal wall thickness to be not less than 0.2 mm. Two dimensional collimation

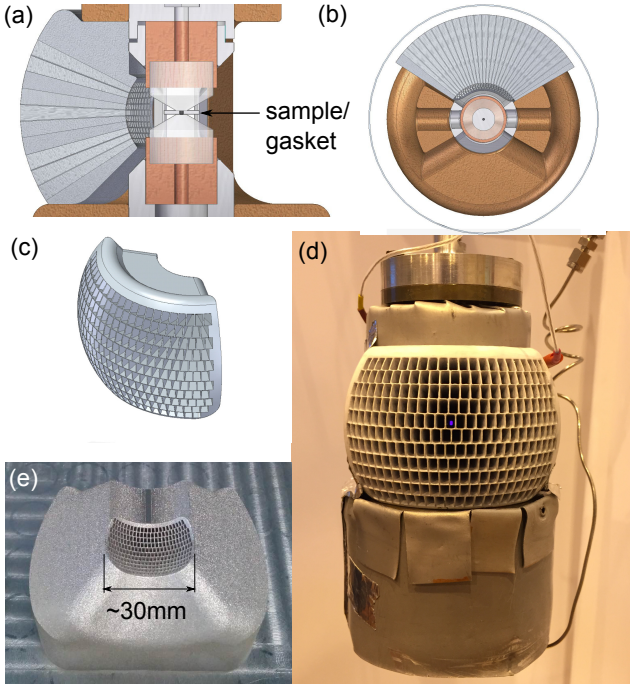

FIG. 5. (a) Vertical and (b) horizontal sections of pressure cell with collimator design, the sample sits between the two sapphire anvils, (b) shows the wall of the 100 mm bore cryostat, (c) CAD model of radial collimator, (d) detector side of printed collimator, coated in Gd_2O_3 paint, and fitted to pressure cell. The sample region can be seen through the collimator illuminated by the laser used for manometry. (e) Sample side view of printed collimator.

was chosen for the first full build of the collimator, as this provides a theoretical advantage over conventional collimator units which cannot angle foils simultaneously in vertical and horizontal planes, and gives the device a more rigid 'comb' structure. It is more common to use a 1D radial collimator with a slit to narrow the incident beam, but 2D collimation has the advantage that secondary scattering events are also effectively collimated. The shape of the device was chosen to be spherical to ensure that the length of each of the channels was identical, to ensure even collimation. The final design is pictured in figure 5.

V. ONLINE TESTING

The collimator unit was tested using the WISH instrument at the ISIS neutron facility. The gasket was made from aluminium, and the sample used for testing was a powder of the perovskite $SrTiO_3$, available from Alfa Aesar. The sample and gasket were placed between two sapphire anvils within the pressure cell, and aligned to be in the vertical plane of the collimator. The sample volume used in the test was approximately 0.25 mm^3, and the count time for the test was 45 minutes. The tests used the symmetry of the cell, and detector layout of WISH to compare data with and without the collimator simultaneously. The raw data from the detector, and the focussed data, with Bragg peaks masked, are shown in figure 6. Some anvil materials used with the pressure cell are not single crystal, and so peak masking is not always possible.

VI. DISCUSSION

The raw data show a clear reduction in the intensity and number of parasitic Bragg peaks contributed from the single crystal sapphire anvils. The focussed data show a large reduction in the incoherent background present in the data, and a reduction in the intensity of the powder peaks of the gasket and sample. Comparing the integrated intensities of the sample and gasket peaks shows that the sample signal becomes approximately 10 times more intense relative to the gasket, with an approximately 96% reduction in aluminium intensity. Analysis of the background signal also shows an increase of signal to noise of approximately 76%. In addition, a number of the weaker parasitic reflections at longer wavelengths are removed from the data completely.

The sample peak intensities, relative to the background in each case, reduce to $\approx 40\,\%$ of the uncollimated levels, which is larger than expected from the simulations. This is partly due to the effects of finite wall thickness, as the foils block the signal over sections of the detectors interrupting the powder rings and reducing the integrated intensities. The angular interruption due to the foil thickness is estimated to be 4° over the 30° out of plane coverage available on WISH, and 20° over the in plane 110° windows on the pressure cell. The reduction in sample peak intensity relative to background is approximately uniform across the detectors, with no peaks completely disappearing, indicating that this loss in sample signal may mostly be due to the inclusion of the vertical collimation. The 2D design presented may therefore be more suitable for use with single crystal samples, where a maximum reduction in powder signal contribution is desired. Another possibility is that the collimator was slightly misaligned when attached to the cell. Due to the need for tight collimation, a misalignment of the focus of the collimator by 0.5 mm could lead to a reduction in intensity of by approximately 40%.

The foils also cast a shadow over the detectors, where parts of the sample are masked slightly at certain angles, beyond the effects of wall thickness. This problem is caused by the foils being angled to a point at the centre of the sample. In cases where the sample is surrounded by mostly empty space, the collimator can be adjusted to minimise this shadowing by increasing the inside diameter of the collimator relative to the diameter of the sample. In the case of pressure cells, reducing the shadowing effect in this way results in a large increase in background from surrounding material. Oscillating the collimator about its axis would average out the effects

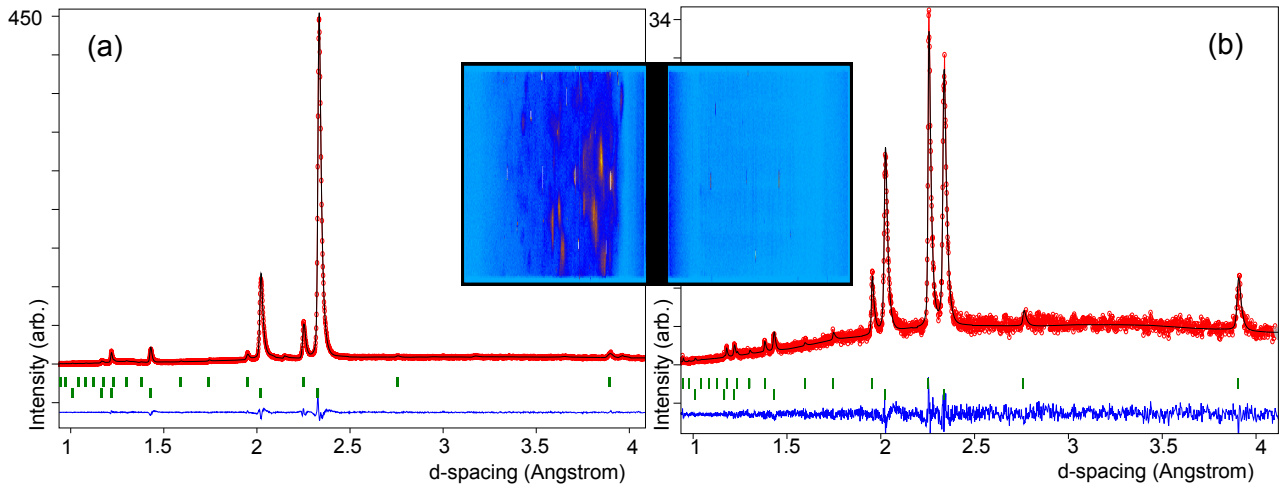

FIG. 6. Focussed diffraction data, with sapphire Bragg peaks masked, taken from the two $2\theta = 90°$ detector banks on WISH at the ISIS facility (a) without collimation, (b) with collimation. The data has been LeBail fit showing the reflections from the $SrTiO_3$ sample (upper ticks) and the Al gasket (lower ticks). Inset, raw unmasked data from detectors, left hand side without collimation, right hand side with collimation. Masking the Bragg peaks is significantly less time consuming with the use of collimation.

of shadowing, but would require a rotational mechanism difficult to implement in a cryogenic environment. Another possibility, only suitable for powder analysis, uses the symmetry of the scattering geometry of the pressure cell. A secondary collimator could be installed on the opposite side of the cell to the primary collimator, with a slightly different spatial layout of channels. The data from both sides of the instrument could then be summed, again averaging out the effects of shadowing certain reflections more than others.

Aside from 2D radial collimation, there are many other collimator concepts which could possibly be manufactured using 3D rapid prototyping. Due to the geometry of the Debye-Scherrer cones formed from powder samples, collimators made from vertical foils are intrinsically less efficient in forward and backscattering angles, being most transmissive at $2\theta = 90°$. For time-of-flight neutron diffraction this is unfortunate, as the resolution is maximised in backscattering. Using 3D printing it may be possible to incorporate a conical form to a radial collimator, where the vertical foils become increasingly curved from the vertical at angles away from 90°. This would dramatically improve the efficiency of the transmission of the collimator in forward and backscattering regions.

Whilst it is possible to simulate a perfect collimator, where the geometry of the collimator is only limited by the ability of the software to incorporate it, the manufacture of such devices is severely limited by machining and assembly capabilities. 3D rapid prototyping is a step towards lifting this limitation, allowing for increasingly complex designs to be manufactured relatively inexpensively.

VII. CONCLUSION

A 3D laser-sintered collimator has been shown to effectively reduce neutron incoherent background, and coherent contributions from the material immediately surrounding the sample. The use of such collimators is very promising for increasing the efficiency of data collection from small samples for neutron scattering experiments, or for improving the data quality collected where sample volume is constrained by the sample environment. Online testing at the ISIS neutron facility has shown that the collimator drastically reduces levels of background signal generated by material directly surrounding the sample. The tests have shown that the sample signal is reduced more than expected due to foils shadowing regions of the sample to the detector. The next iteration of the design will use 1D collimation, attempting to reduce the wall thickness to 0.1 mm in order to reduce sample losses to the collimator, and will use a larger angular separation to reduce shadowing effects. In addition, neutron transmission measurements will be performed to further characterise the efficiency of the collimator.

Achieving efficient collimation is challenging, with there being a need to tailor specific collimators to individual measurements; for example the optimal geometry differs between single crystal and powder samples or for the incorporated sample environment, different sample volumes, or different detector layouts. The demonstrated effectiveness of 3D rapid prototyping in collimator manufacture is promising for the development of individual collimation units for experiments without the need to alter the existing setup of the instrument. Compact devices can be incorporated in existing sample environment, such as being installed in the jacketing of cryostats, or within

larger existing collimators, which many instruments are already able to accommodate.

ACKNOWLEDGMENTS

The authors would like to thank Daniel Kirk and his collaborators from CRDM Ltd. for their advice and assistance with the printing of the collimator, and Lino D'Ambrogio from Euro Collimators Ltd. for his assistance in coating the parts. This work was funded and supported through STFC studentship and EPSRC grant EP/J00099X.

[1] S. Klotz, *Techniques in high pressure neutron scattering.* (CRC Press, Taylor & Francis Group, Boca Raton, Florida, 2013).
[2] S. Qiu, J. Yu, G. Zhu, O. Terasaki, Y. Nozue, W. Pang, and R. Xu, Microporous and Mesoporous Materials **21**, 245 (1998).
[3] J. R. Santisteban, M. R. Daymond, J. A. James, and L. Edwards, Journal of Applied Crystallography **39**, 812 (2006).
[4] R. Boehler, M. Guthrie, J. Molaison, A. dos Santos, S. Sinogeikin, S. Machida, N. Pradhan, and C. Tulk, High Pressure Research **33**, 546 (2013), http://dx.doi.org/10.1080/08957959.2013.823197.
[5] C. Petrillo, E. Guarini, F. Formisano, F. Sacchetti, E. Babucci, and C. Campeggi, Nuclear Instruments and Methods in Physics Research Section A: Accelerators, Spectrometers, Detectors and Associated Equipment **489**, 304 (2002).
[6] J.-L. Mutz, O. Bonnet, R. Fairbend, E. Schyns, and J. Seguy, in *Integrated Optoelectronic Devices 2007* (International Society for Optics and Photonics, 2007) pp. 64790F–64790F.
[7] A. S. Tremsin, D. F. Mildner, W. B. Feller, and R. G. Downing, in *Nuclear Science Symposium Conference Record, 2003 IEEE*, Vol. 1 (IEEE, 2003) pp. 503–507.
[8] S. W. Wilkins, A. W. Stevenson, K. A. Nugent, H. Chapman, and S. Steenstrup, Review of Scientific Instruments **60** (1989).
[9] M. Zhong, W. Liu, G. Ning, L. Yang, and Y. Chen, Journal of Materials Processing Technology **147**, 167 (2004).
[10] X. Yan and P. Gu, Computer-Aided Design **28**, 307 (1996).
[11] M. Agarwala, D. Bourell, J. Beaman, H. Marcus, and J. Barlow, Rapid Prototyping Journal **1**, 26 (1995), http://dx.doi.org/10.1108/13552549510078113.
[12] M. K. Jacobsen, C. J. Ridley, A. Bocian, O. Kirichek, P. Manuel, D. Khalyavin, M. Azuma, J. P. Attfield, and K. V. Kamenev, Review of Scientific Instruments **85**, 043904 (2014).
[13] Oracle, "JAVA SE, version 1.8.0," `https://www.oracle.com/java/index.html`, online; accesed August 2015.
[14] K. Lefmann and K. Nielsen, Neutron News **10**, 20 (1999), http://dx.doi.org/10.1080/10448639908233684.
[15] P. Andersen, K. Lefmann, L. T. Kuhn, P. Willendrup, and E. Farhi, Physica B: Condensed Matter **350**, E721 (2004), proceedings of the Third European Conference on Neutron Scattering.
[16] D.-Q. Wang, X.-L. Wang, J. L. Robertson, and C. R. Hubbard, Journal of Applied Crystallography **33**, 334 (2000).